

6.0 Results of Aviation Receiver Testing

6.1 PRF Comparisons

One of the fundamental parameters which can be varied for the UWB signal is the Pulse Repetition Frequency (PRF). Figure 14 shows the results for unmodulated UWB tests for various PRFs between 100 kHz and 20 MHz. Note that the curves are overlaid upon that obtained for broadband noise which was originally depicted in Figure 11. This allows each of the UWB test cases to be compared to the broadband noise.

From Figure 14, it is possible to draw some initial conclusions regarding the impact of the PRF relative to white noise. The results initially appeared to suggest that when the PRF is high (5 – 20 MHz), the impact of UWB was similar to that of broadband white noise. When the PRF was lower (100 kHz – 1 MHz), the impact of UWB decreased, as may be suspected as the GPS signal is designed to be robust against pulsed interference. When the PRF is low, each UWB pulse has sufficient separation from each other; thus the impact to GPS is small. It is important to recognize that this is the case for a single UWB emitter, no attempt to quantify aggregate effects has been done thus far. It is speculated that the aggregate impact from multiple unsynchronized UWB emitters at low PRFs will have the potential to combine in time, eliminating the desired “pulsed appearance” of a single low-PRF UWB emitter.

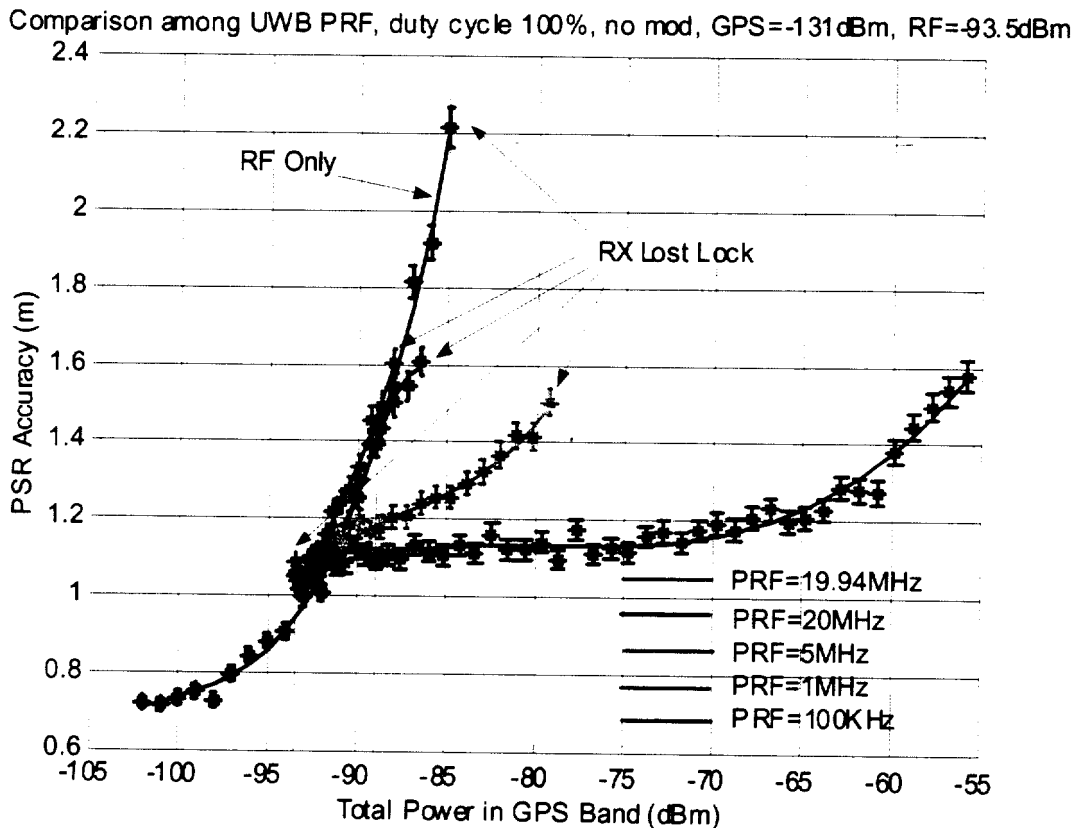


Figure 14: Comparison of UWB for Different PRFs

However, a closer inspection of the results in Figure 14 lead to some inconsistencies regarding the initial conclusions. Originally, it was suggested that the high (5-20MHz) PRFs impacted performance very similar to the effect of broadband white noise as the accuracy curves follow that obtained using only broadband white noise. However, the tests were allowed to continue beyond the accuracy requirement to the point at which the receiver lost lock or full UWB power was entering the receiver. In all cases except that for the lower PRFs, the receiver lost lock at a significantly lower total UWB + broadband white noise power level than that obtained using broadband noise alone. This is true even though the high-PRF curves initially appear to closely follow that result obtained for broadband white noise. Even more troubling was the case for a PRF of 19.94 MHz, a value that is very close to the 20 MHz case yet has significantly worst performance. The 19.94 MHz case lost lock almost immediately at the power level at which the UWB waveform was first introduced.

As a result of the inconclusive results obtained from looking solely at the accuracy measurement, it was necessary to expand the investigation to attempt to explain and validate the results obtained. In order to do so, the next step was to attempt to characterize the waveform in the time and frequency domains. The time domain depiction of the UWB pulse was well understood based on the initial analysis of the pulse as it proceeded from the pulsar through the additional RF components. This provided the insight that lower (under 1 MHz) PRFs would likely appear as pulsed interference and would have a reduced impact on GPS performance. This was justified in the results. Unfortunately, the time domain representation does little to explain the widely varying performance when small changes are made to the PRF. In order to better understand this aspect, it was necessary to employ to a frequency domain representation of the various UWB signals.

6.2 Frequency Domain Representation of the UWB Waveform

The time domain representation of the resulting UWB pulse provided a basis for the performance difference observed between high and low UWB PRF impact on the GPS signal. However, it did nothing to explain why slight differences in the higher PRFs resulted in significant variations in the results from Figure 14. The frequency spectrum for the UWB waveform was not unknown. Results had been presented previously [9], including its representation, and those early depictions were included as Figure 5 in Section 3.0 of this report. The goal here is to focus specifically on the spectrum of the UWB waveform which will overlap with the GPS spectrum and attempt to explain the results obtained in Figure 14. This will be the focus of the results presented.

However, there is a potential consequence of the using the reduced observation window. This window corresponds to the L1 bandpass filter (see Figure 13) which has been included to focus on the spectrum within the GPS band and obtain accurate power measurements. Most GPS receivers will utilize a multistage frequency plan with the components nearest the antenna being the widest bandwidth to minimize cost. It is possible these first wider bandwidth stages could receive a substantial increase in UWB energy over what is tested with the inclusion of the L1 test bandpass filter, which may saturate the amplifier and make it inoperable until it can recover from this state. This aspect has not been tested within these experiments as, again, the L1 test bandpass filter was used to provide an accurate power measurement and to focus the observation interval, but it is important to note the potential for further degradation in GPS performance.

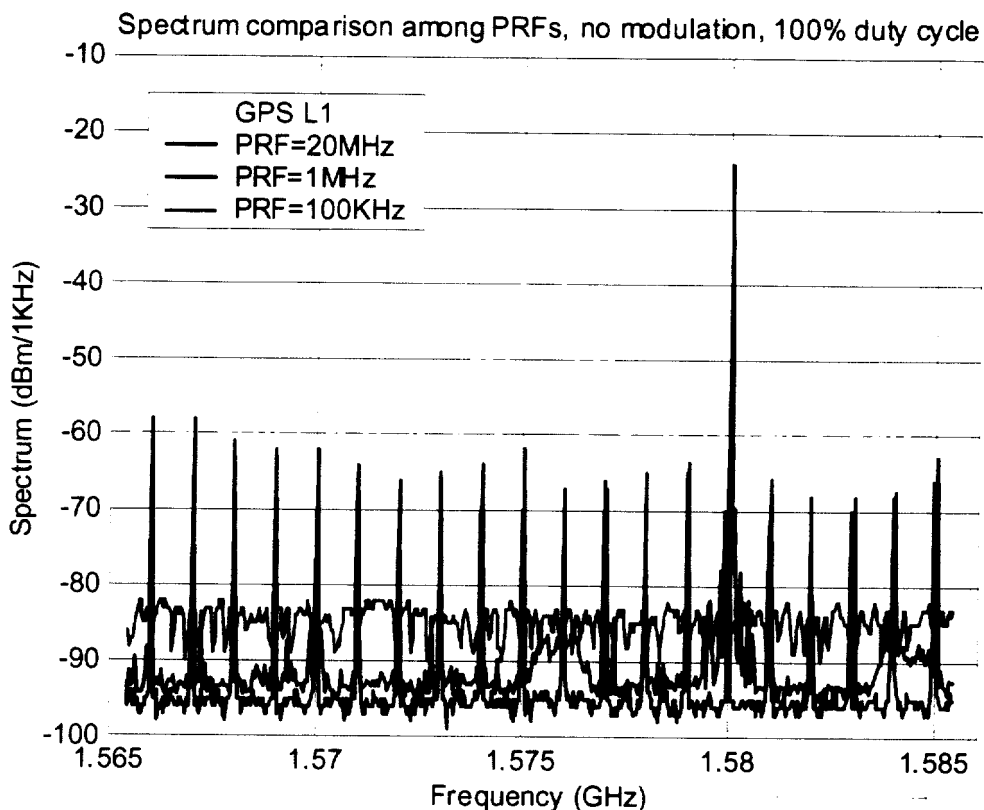


Figure 15 shows the spectrum of three different PRFs for UWB waveforms that would enter the L1 filter in the test setup. The spectrum for the GPS signal has been overlaid on the plot to provide a sense of the frequency span under scrutiny. No attempt has been made to indicate relative power levels between the GPS spectrum and that of the UWB spectra. The relative power levels of the UWB spectra are correct but do not directly correspond to the levels entering the receiver, as the measurement is taken prior to the variable attenuator in order to provide a measurable reading.

The first aspect to notice in Figure 15 is the spectral lines for each of the waveforms. The 20 MHz PRF has a predominant spectral line at 1.58 GHz. This is a direct result of the 20 MHz PRF for the unmodulated UWB pulse. Referring back to Figure 5 which showed the spectrum for the same signal taken over a wider bandwidth with a wider resolution bandwidth, it becomes clear that Figure 15 is a zoomed and refined view of that originally displayed in Figure 5. Also in Figure 15 is the spectrum for the other PRFs. The 1 MHz PRF has multiple spectral lines of approximately equal power. These lines are at 1 MHz intervals, the same as the PRF, across the frequency span under observation. Finally the 100 kHz PRF UWB spectrum appears to be the only one shown that does not display distinct spectral lines. This lack of spectrum lines for this case is only a result of the wide bandwidth displayed in the above plot. The spectrum for the 100 kHz PRF UWB waveform is indeed represented by spectral lines spaced 100 kHz apart. As such, they become denser with lower power in each line and are thus indistinguishable in Figure 15.

This figure immediately provides some insight into the expected impact a UWB emitter will have on GPS. Although all UWB signals have a wide bandwidth, the unmodulated high PRFs produce distinct spectral lines in the GPS band. Thus the impact of the UWB waveform on GPS performance cannot be equated with additional broadband noise. Instead it will be a combination of additional broadband noise and discrete spectral lines. Stated more accurately, a UWB emitter when radiating into the GPS band will produce the combined effect of a higher thermal noise floor and Continuous Wave (CW) interference at frequencies determined by the PRF of the UWB emitter. Although insightful, Figure 15 does not definitively indicate the performance difference experienced when the UWB PRF varies slightly between 20 MHz and 19.94 MHz. Prior to looking at the spectral plot for 19.94, accuracy results for an additional point around 20 MHz was investigated, and this result is shown in Figure 16.

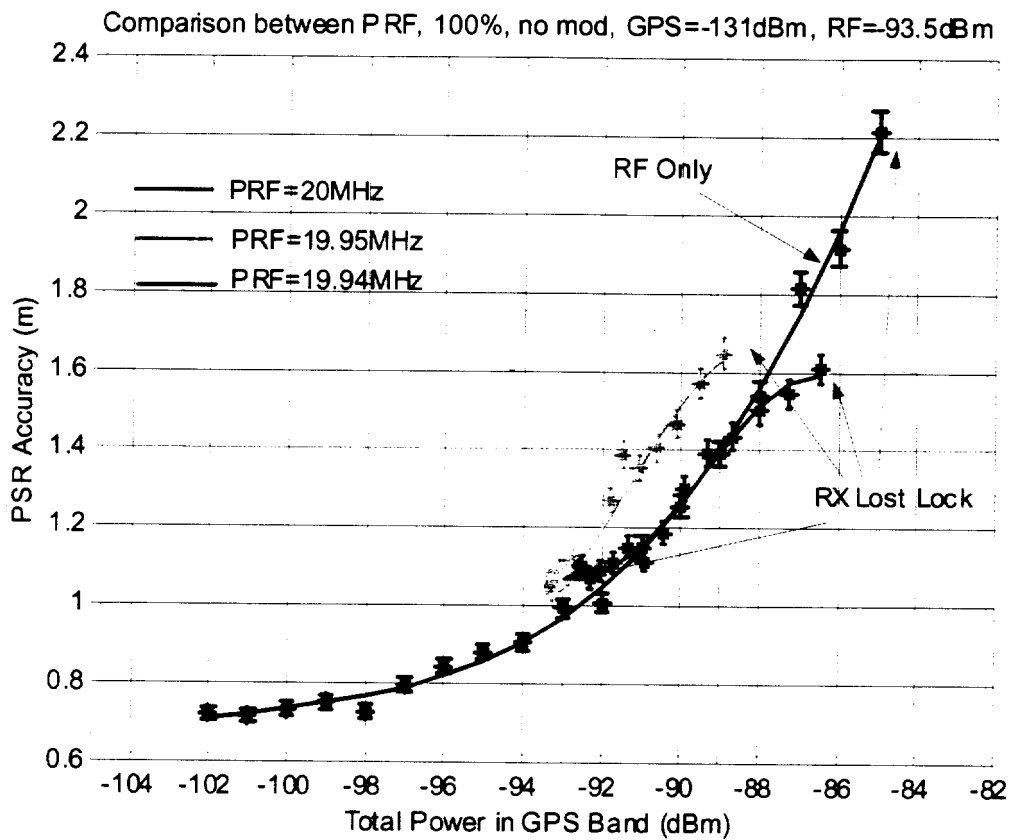


Figure 16: Accuracy Comparison among PRF = 20 MHz, 19.94 MHz, and 19.95 MHz

The tests with PRFs of 19.94 MHz and 20 MHz were conducted along with a PRF of 19.95 MHz and the accuracy result varied significantly, much greater than might be initially expected from such a small change in the PRF. As an attempt to understand the performance, the spectrum for the UWB signal with these three PRFs was generated and is included in Figure 17.

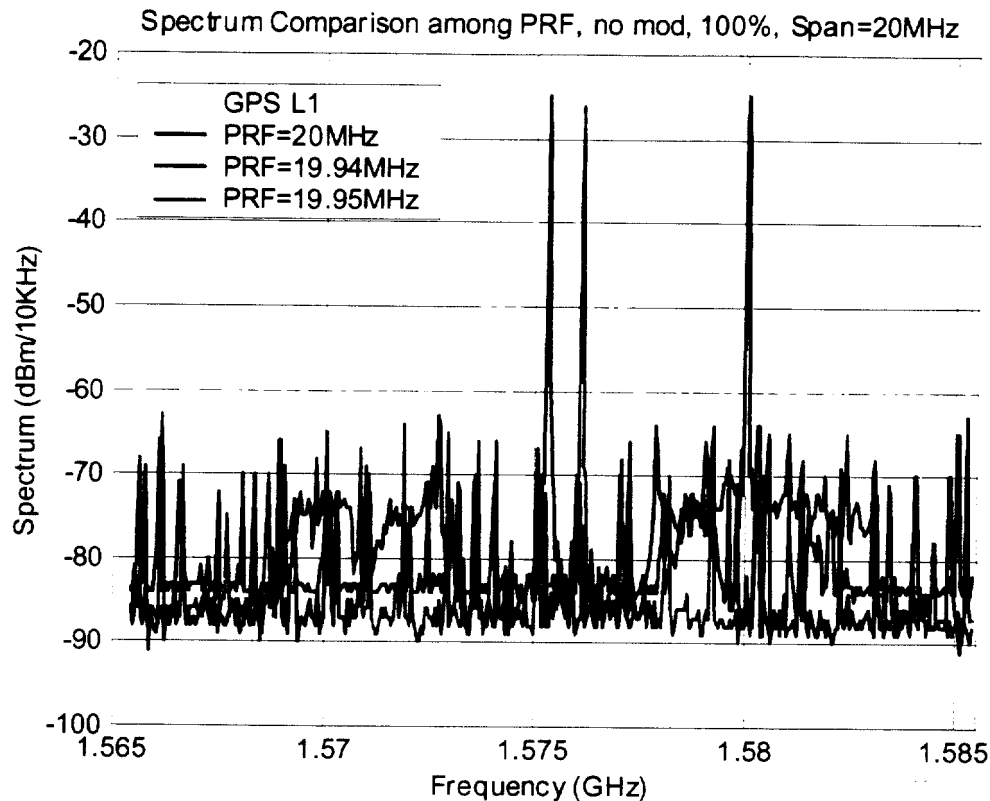


Figure 17: Spectrum Comparison among PRF = 20 MHz, 19.94 MHz, and 19.95 MHz

The most damaging result, which was an almost immediate loss of lock, occurred for a PRF of 19.94 MHz. It is clear from Figure 17 that a large spectral spike hits the peak of GPS L1 main lobe when the UWB PRF = 19.94 MHz. This spike hits the side of the main lobe when PRF = 19.95 MHz and hits at about the 5th sidelobe when the PRF = 20 MHz. This explains why the PRF = 19.94 MHz case does the most severe damage to GPS – the receiver loses lock (making the satellite unusable) well before the accuracy requirement is broken. The 19.95 MHz PRF is less threatening, as it leads to violation of the accuracy requirement at a total interference power of -90 dBm and then causes loss-of-lock at -88 dBm. The PRF = 20 MHz case has the smallest impact among these three cases, as it is about 2 dBm better than the 19.95 MHz case. This indicates that these higher PRFs do not impact the receiver solely as increased thermal noise but rather as a combination of thermal noise and discrete line spectra.

In general, spectral lines and CW interference are more damaging to the GPS receiver than increased broadband white noise interference. This data shows approximately a 9 dB penalty for CW interference when compare with broadband noise performance in regard to its impact on the GPS receiver. This is consistent with the 10 dB distinct made for different masks for broadband and CW interference in [3] and helps validate our theoretical performance expectations.

From these results, UWB emitters with these PRFs raise the thermal noise floor, but also generate CW spikes in the frequency spectrum, both of which impact the GPS receiver

performance. A minimal impact from a UWB emitter would be expected if there were no distinct spectral lines in the resulting frequency spectrum, but there would still be the consequence of an increased noise floor. If the UWB emitter is to generate such distinct spectral lines as has been the case for all the constant PRFs tested, the interference will be more like a combination of increased broadband noise combined with the more damaging CW interference. Thus, the decreased margin between accuracy measurements and loss of lock (depicted in Figure 14) for UWB emitters when compared with broadband noise can be attributed to this CW interference profile of the UWB spectrum.

Note that for any practical UWB transmitter, some variation around the nominal UWB PRF is unavoidable due to imperfect clock components. Thus, a transmitter designed with a 20 MHz PRF may wander over to 19.94 MHz (a difference of only 0.3%) and cause loss of GPS satellite tracking. Loss of tracking is even worse for GPS than violation of the accuracy requirement for precision users, as it affects all users of GPS and makes it very difficult for precision users to meet their continuity (loss of navigation) requirement.

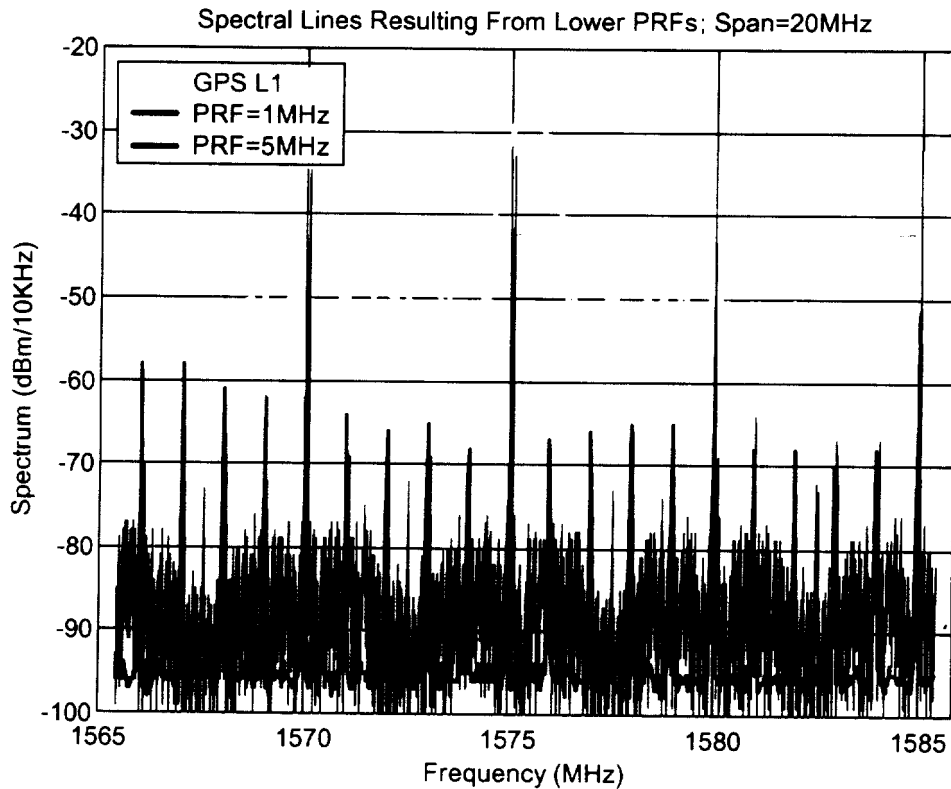


Figure 18: Spectrum Comparison for PRFs of 5 MHz and 1 MHz

It is quite simple to predict the location of the spectral lines given the PRF. If the PRF is n MHz, then there will be resulting spectral lines at: $n, 2n, 3n, 4n, \dots$. If the PRF is sufficiently high, these spectral lines will be distinct and contain significant energy. If the PRF is relatively

lower, on the order of 1 MHz or less, these spectral lines are much more dense. For example, a PRF of 20 MHz implies distinct spectral lines will occur at one location within the bandwidth of the L1 bandpass filter, specifically at 1580 MHz, which is the base PRF multiplied by 79. This location is verified in Figure 18. If the base PRF is set to 19.94 MHz, the inband spectral line occurs at 19.94 MHz multiplied by 79 or 1575.26 MHz, which is again validated in Figure 18. Thus it becomes possible to predict where the distinct spectral lines will occur. If the PRF is 5 MHz, the distinct spectral lines would be expected at: 1570, 1575, 1580, and 1585 MHz in a 20 MHz span about the GPS center frequency. If the PRF is 1 MHz, then spectral lines will occur inband at 1566, 1567, 1568, ... 1583, 1584, and 1585 MHz. This is confirmed in Figure 18.

It is important to note that all nominal UWB PRF's of 5 MHz and above tested without modulation have similar "weak points" in regard to their ability to minimize interference to GPS. That is, there will always be a PRF near the nominal PRF that will cause a spectrum line to fall in the main GPS lobe, leading to rapid loss of lock. For a 20 MHz PRF, the problematic case is 19.94 MHz as has been shown above. A PRF of 15.0 MHz results in a damaging spectral line at 1575 MHz without any clock adjustment. A PRF of 10 MHz initially appears to have minimal impact to GPS, as its nearby spectral lines are located at 1570 and 1580 MHz. However, a slight change in the 10 MHz PRF to 9.97 MHz will result in a spectral line at 1575.26 MHz, which is the 9.97 MHz base PRF multiplied by the integer multiple 158. UWB designers must take steps to remove the possibility of spectral lines overlapping the GPS band in this manner, as it is exceptionally damaging for GPS performance.

The last issue within this section on spectral lines concerns the width of the resulting UWB spectral lines themselves. Although GPS appears to have the sinc function spectrum depicted in the above figures, it is actually comprised of the distinct spectral lines enveloped in the sinc function [11]. The spectral lines of GPS are 1 kHz apart and result from the periodic nature of the GPS C/A code. As a result of the cross correlation properties of the C/A code, certain GPS spectral lines are more important than others, as they contain more energy. A question arises with respect to the UWB interfering spectral lines – Are the resulting UWB spectral lines truly lines interfering with a single GPS spectral line? Or do the UWB spectral lines have some width and impact multiple GPS spectral lines? In order to address this question, it was necessary to utilize a very narrow resolution bandwidth for the observation window. In Figure 19, these questions are addressed as the spectrum for a 15.91 MHz PRF is overlaid with that for the GPS signal across a 10 kHz bandwidth. It is easy to compute the position of the 15.91 MHz spectral line, in this case it is at a multiple of 99 times the base PRF, or 1575.09 MHz. In the figure, it is clear that the UWB spectral lines have some finite width relative to the GPS spectral lines - the UWB spectral line typically covers 2-3 GPS spectral lines. The finite width of the UWB spectral lines most likely results from clock jitter or other component instability. Nevertheless, it is possible to state that the sensitivity of GPS to UWB interference depends on where the UWB spectral lines lie within the GPS spectrum, not which specific spectral line of GPS is overlapped based on Figure 19.

This section is one of the most important products of our UWB testing, as it provides a means to predict GPS performance in the presence of UWB. Under the best possible circumstances, UWB can only be expected to raise the noise floor in the GPS receiver. It is important to note that raising the noise floor is by no means a trivial or desired consequence, rather it is quite damaging as it will have a negative impact on performance. But this elevation in the noise floor is the best that could be expected. If the UWB waveform parameters result in the generation of distinct spectral lines, the UWB signal will be more damaging to the GPS signal than elevated noise levels – it will result in an early loss of lock. The PRF is directly related to the position of the spectral lines; thus it should be possible to predict performance based on this

parameter. The testing of other parameters, which are reported in subsequent sections, can at best be attempts to modulate the UWB waveform so that its spectrum appears more like broadband noise rather than resulting in distinct spectral lines. If threatening spectral lines are removed, GPS performance should mimic the broadband noise curve and is the best that can be expected for relatively high PRFs greater than 1 MHz which will not appear as pulsed interference to the GPS receiver.

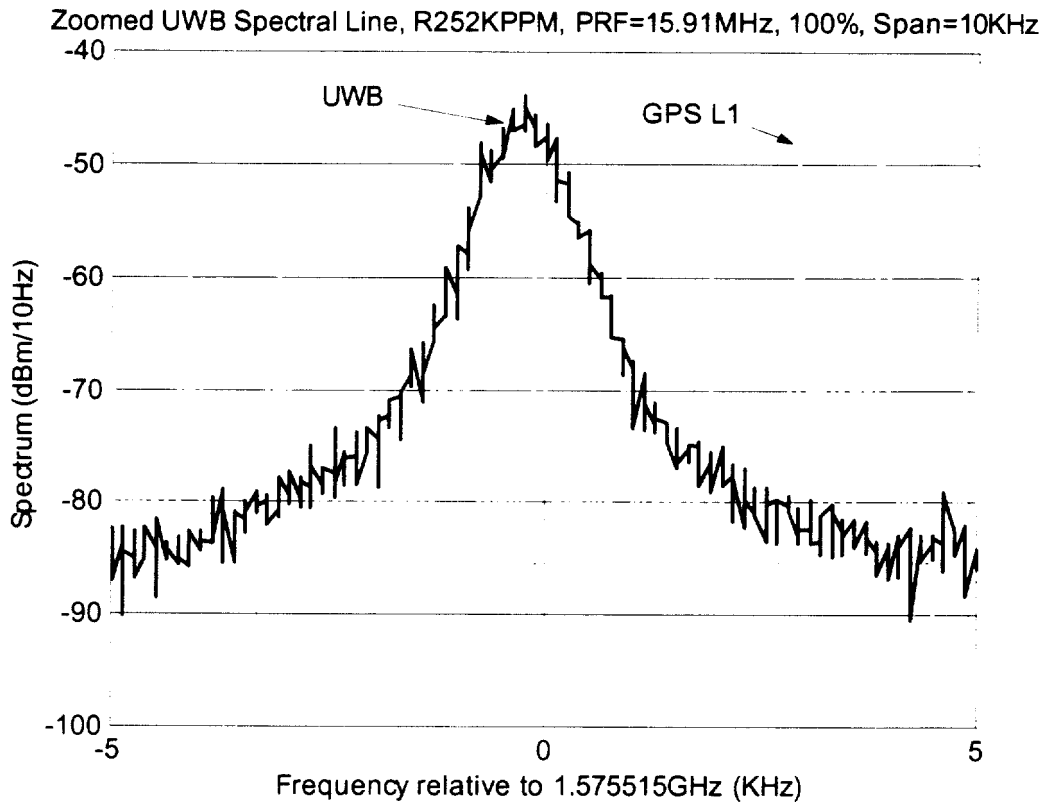


Figure 19: Zoomed-in View of UWB Spectral Lines

6.3 Comparison of UWB Duty Cycles

For a fixed PRF of 20 MHz, tests were run with duty cycles of 100%, 50%, and 10%, and the results are compared in Figure 20. The difference between 100% and 50% is fairly minor, while a 10% duty cycle has much smaller impact on GPS than the higher duty cycle cases tested. Note that the UWB power in the GPS band has been normalized. In other words, the UWB power in the GPS band for a given x-axis value is the same for all three cases. Also note that when the PRF is changed from 20 MHz to 19.94 MHz, the receiver lost lock at lower UWB power level even for the 10% duty cycle case. This indicates that the GPS receiver remains vulnerable to overlapping spectral lines even for low duty cycles.

With a fixed PRF and duty cycle, the UWB transmitter can be set to different burst-on times, or different pulse periods. This parameter also effects the impact on GPS, as shown in Figure 21. This figure compares the impacts on GPS of burst-on times of 10 μ s, 1 ms, and 10 ms for a 50% duty cycle. It appears that increasing the burst-on time helps reduce the impact of UWB on GPS. It is suspected that increasing the burst-on time (yielding longer periods) yields denser but smaller spectral lines in the sensitive GPS L1 band, thus the harm to GPS is less severe. Also note that the overlapping spectral lines of the PRF = 19.94 MHz case remain damaging.

6.4 Pulse Position Modulation (Random PPM)

In order to test the capability of pulse position modulation to reduce the impact of UWB on GPS, a ten-position modulated case was constructed as illustrated in Figure 22. The pulse will randomly take one of ten positions: the early positions ($-d$ to $-5d$), the nominal position, or the late positions ($+d$ to $+4d$). The minimum separation of two pulses is 50 ns (this is limited by the capability of the pulser in our test setup). A sequence of 250,000 points was constructed. The maximum PRF that can be supported is 2 MHz, which yields $d = 50$ ns with a clock frequency of 40 MHz. The ratio of position dithering was from -50% to $+40\%$. The test results are shown in Figure 23. Since there are ten evenly-spaced positions for each nominal pulse location, when the PRF is set to 2 MHz, the actual spectral lines would look as if the PRF were 20 MHz in the no-modulation case. But each pulse position only has one chance in ten to actually happen; thus the spectral spikes are much smaller (~ 20 dB lower) and the noise floor is higher, as shown in Figure 24.

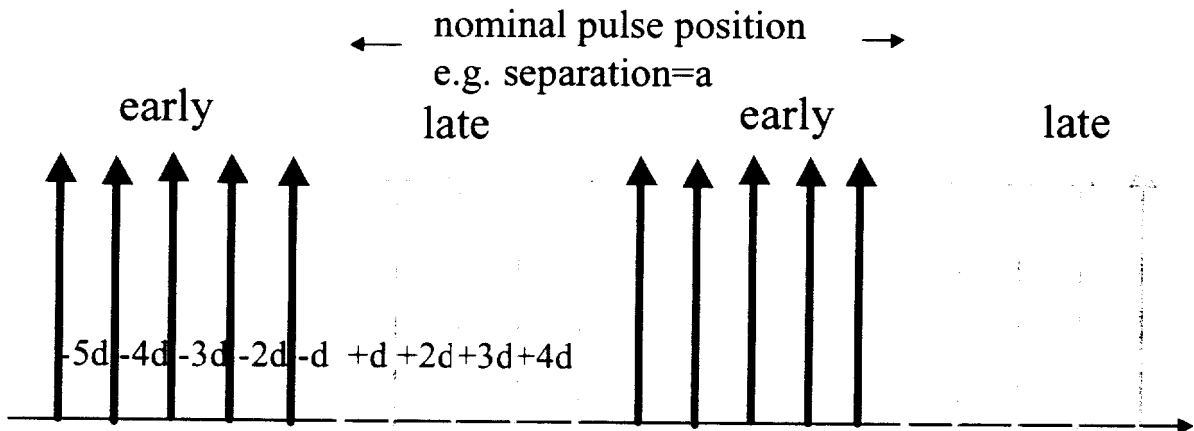


Figure 22: Ten-Position Random PPM

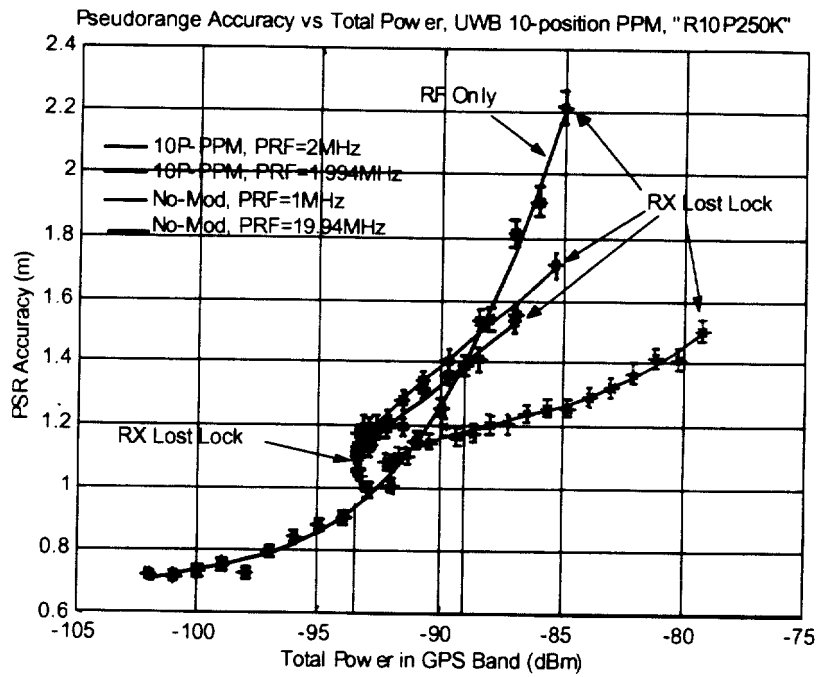


Figure 23: Test Results for Ten-Position PPM

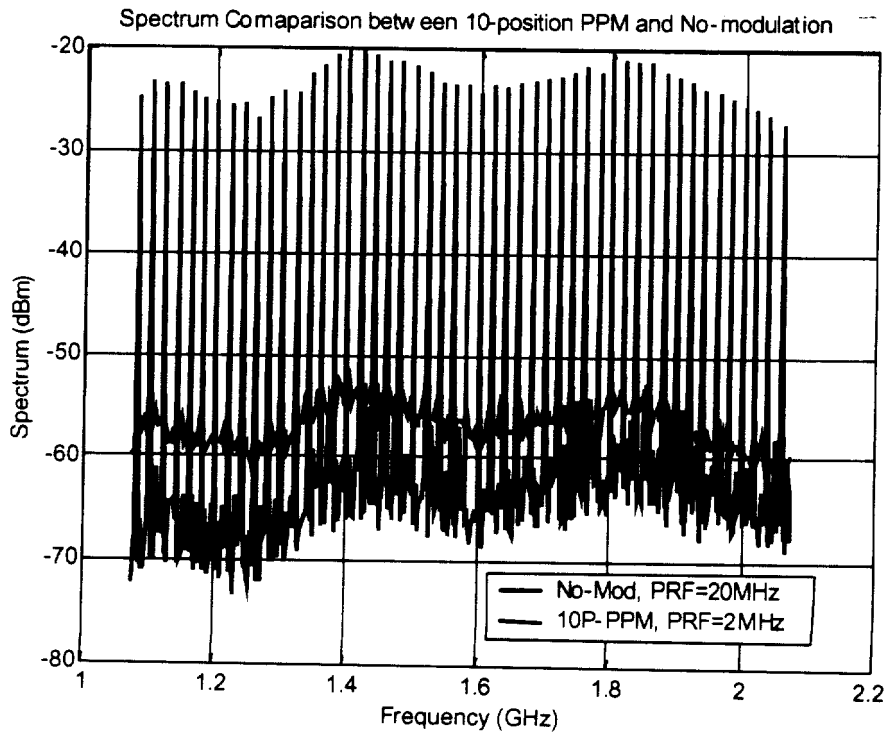


Figure 24: Spectrum Comparison between Ten-Position PPM and No Modulation

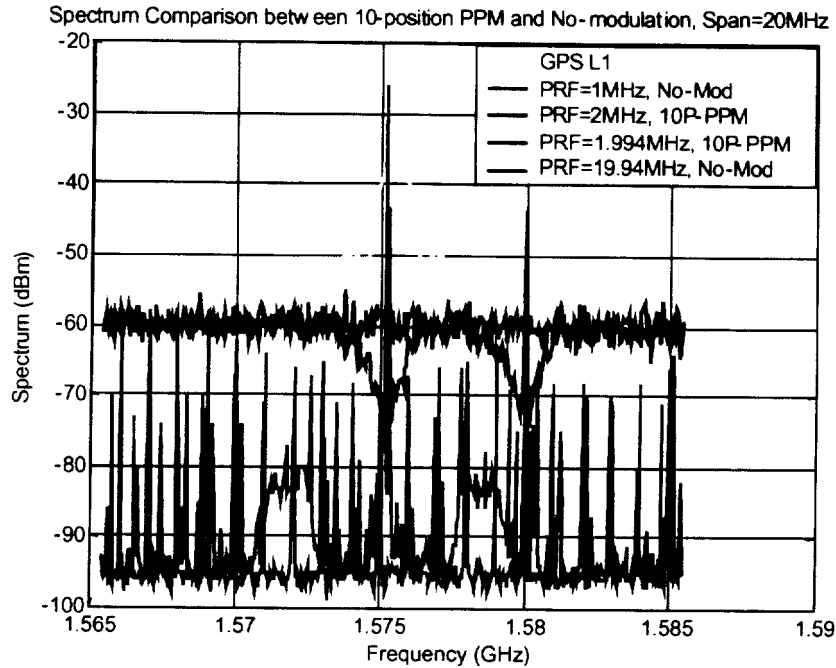


Figure 25: Spectrum Comparison between Ten-Position PPM and No-Modulation in GPS L1 Band

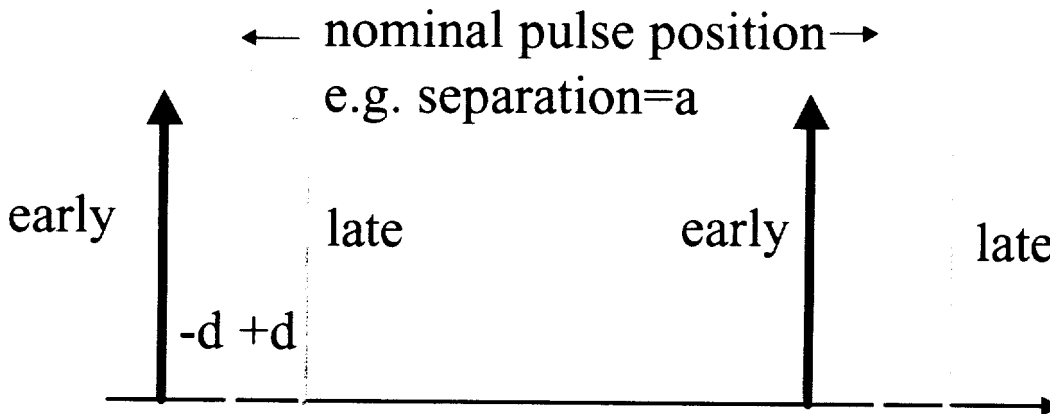


Figure 26: Two-Position Random PPM

From the zoomed-in spectrum comparison of Figure 25, we can more easily understand the results in Figure 23. Though the spike of the PRF = 1.994 MHz case overlaps the GPS main lobe, its strength is 18 dB less than that for PRF = 19.94 MHz in the no-modulation case; thus the impact to GPS is much less severe. The lower magnitude of these spikes makes the exact location of the spikes less important, which explains why the 2 MHz PRF and 1.994 MHz PRF cases yield similar results. These impacts are worse than that obtained for lower PRF in no-modulation case (1 MHz is shown in the plot), as the 1 MHz no-modulation PRF case has spikes near L1 that are suppressed even further beyond those of the two ten-position PPM cases.

A two-position random PPM scenario was also created and is illustrated in Figure 26. The pulse takes either the early position (nominal $-d$) or the late position (nominal $+d$). The minimum separation of two pulses is 50 ns as in the ten-position case. A sequence of 252,000 points was constructed with $d = 2$ ns and $a = 56$ ns when the clock frequency is 250 MHz. The ratio of position dithering (d/a) is $1/28$ (3.57%). The relation of PRF/clock frequency is $1/14$. The test results are plotted in Figure 27. From this plot, the impact of UWB to GPS (from most severe to least severe) is 15.91 MHz, 16.08 MHz, 15.93 MHz, 15.94 MHz, and 15.92 MHz. Figure 28 and 29 show the UWB spectra of these PRFs relative to the GPS L1 band. The order of the power level where the UWB spectral peak hits the GPS spectrum matches the above order very well. This is explained to a large degree by viewing the UWB spectral lines relative to the GPS spectrum near L1.

6.5 Random On-Off Key (OOK) Modulation

In random on-off-key (OOK) cases, the UWB pulses retain their nominal positions, but each individual pulse is turned on or off randomly. This pattern is illustrated in Figure 30. The pulse train is evenly spread. Each pulse is randomly set to be on or off with a 50% probability. The minimum separation of two pulses is 50 ns as noted before. A sequence of 256,000 points was constructed with $d = 50$ ns and a clock frequency of 40 MHz was utilized.

The test results and the resulting spectra for OOK modulation are shown in Figures 31, 32 and 33. Not surprisingly, the location of the UWB spectral lines explains these results. When these lines hit the main lobe of GPS L1 (the 19.94 MHz PRF case), the UWB still has a significant impact on GPS. Compared to the no-modulation scenario with the same PRF, the GPS

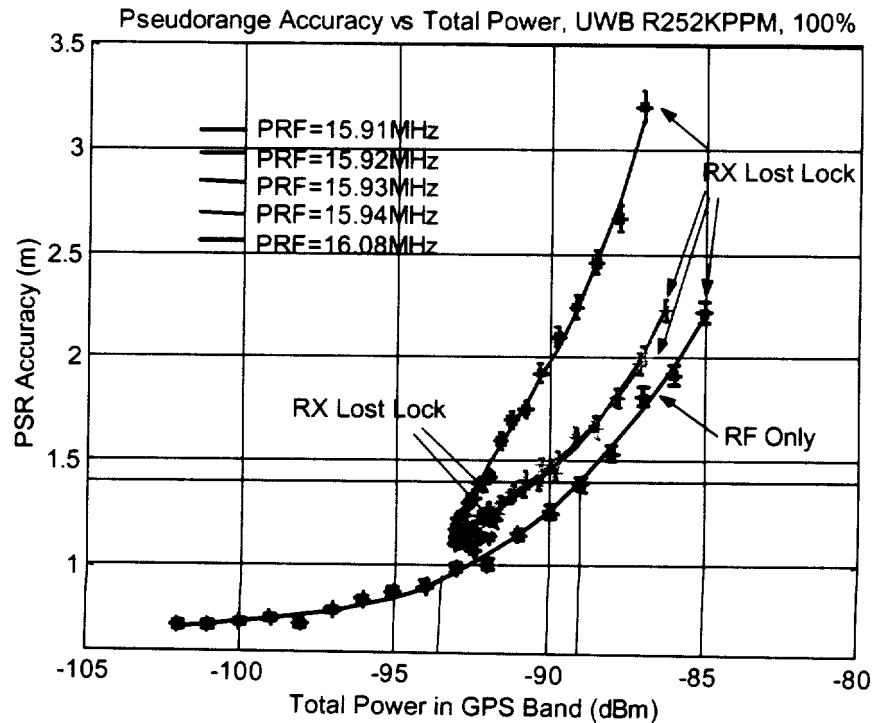


Figure 27: PRF Comparison with Two-Position PPM

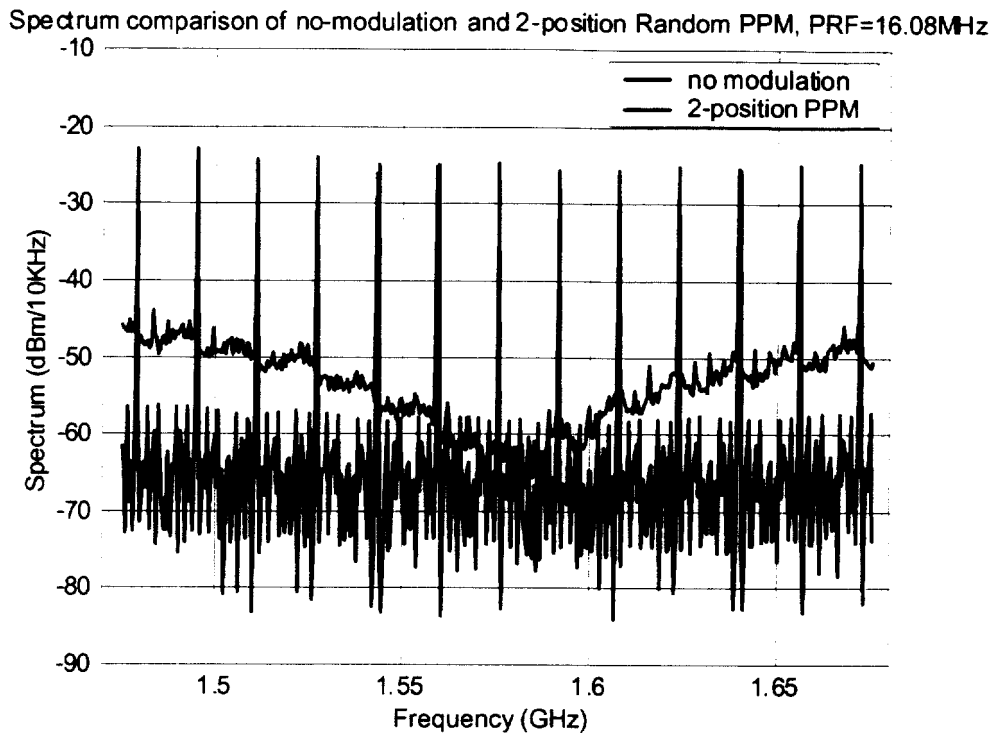


Figure 28: Spectrum Comparison between Two-Position PPM and No-Modulation

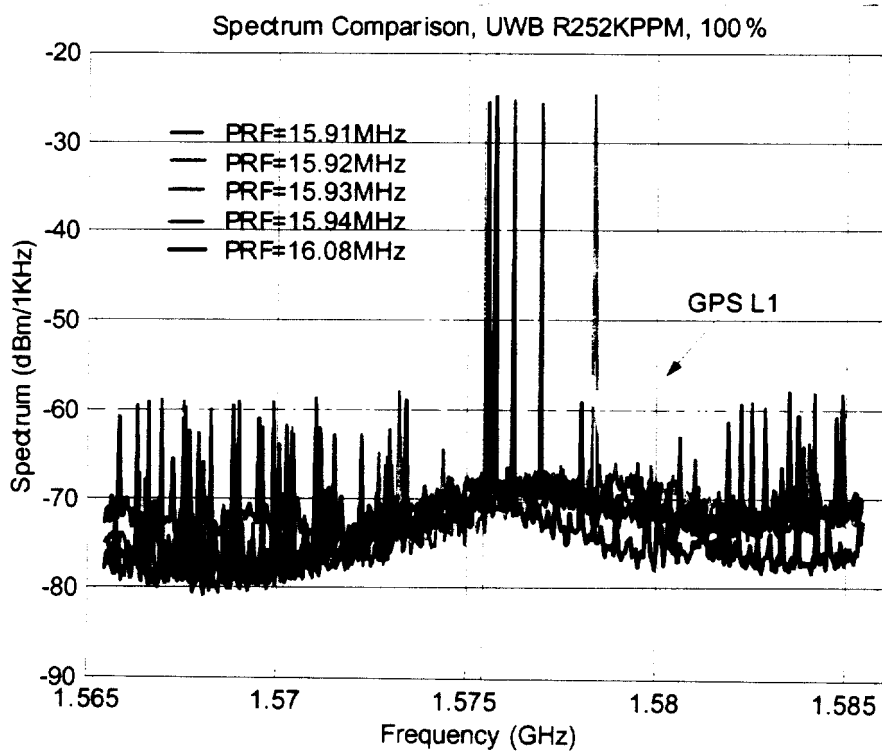


Figure 29: Spectrum Comparison among PRFs with Two-Position PPM

receiver survives slightly better with random OOK. The reason is that with this type of modulation, the spectral lines retain the same positions, but their strength becomes smaller, and the spike "noise floor" moves higher. In other words, OOK modulation makes UWB behave a little more like white noise than the no-modulation cases (see Figures 31 and 32 for details), but a significant gap remains. A 50% duty cycle with random OOK modulation was also tested. The difference between 100% and 50% duty cycles with OOK is similar to the difference between 100% and 50% duty cycles without modulation.

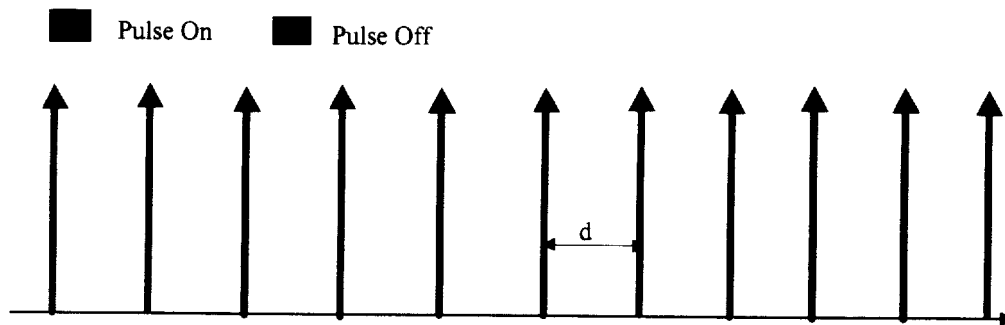


Figure 30: Random OOK Illustration

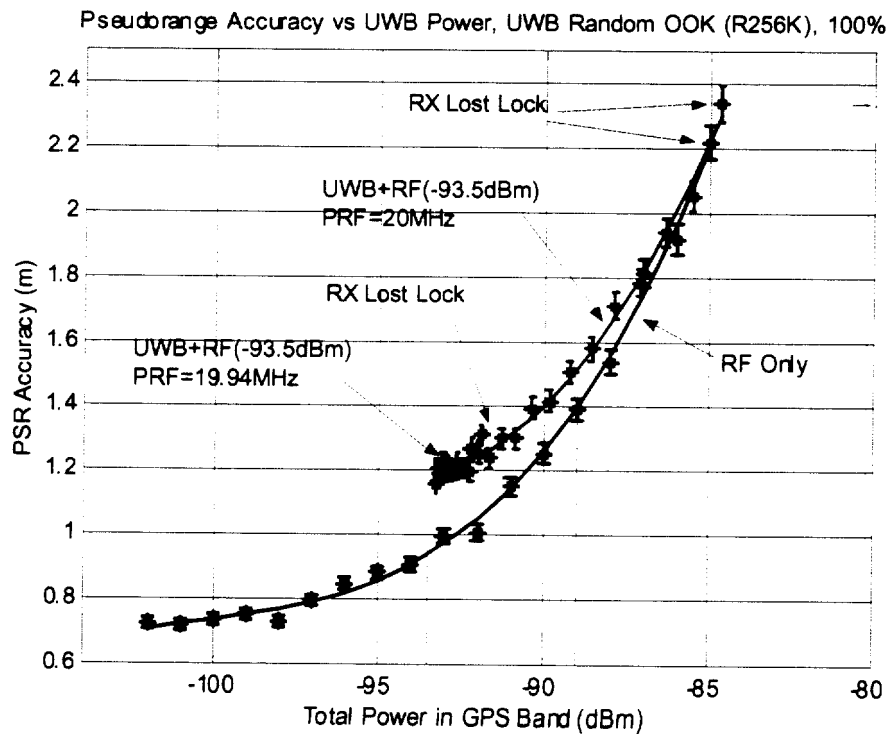


Figure 31: Accuracy Test Results for Random OOK

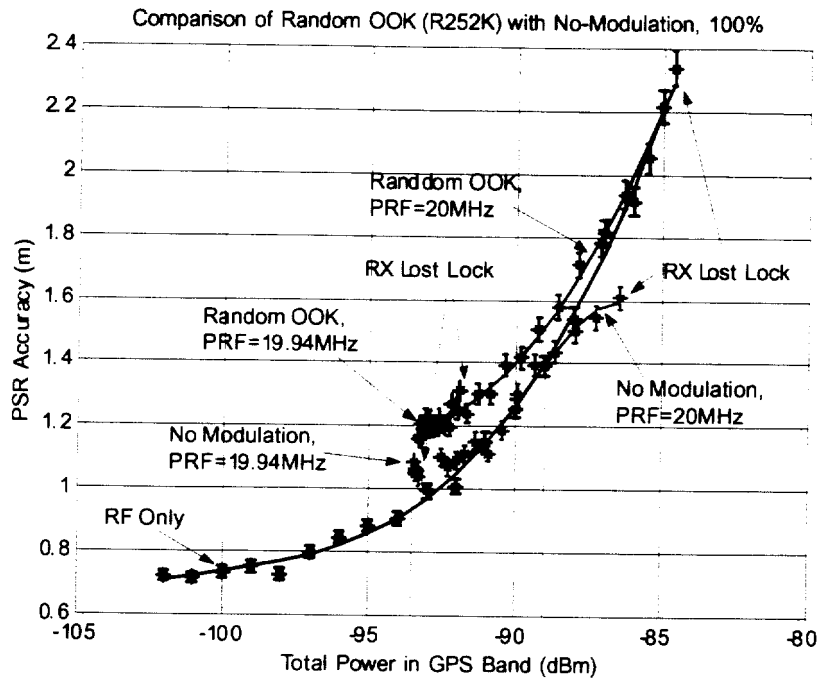


Figure 32: Accuracy Comparison between Random OOK and No-Modulation Cases

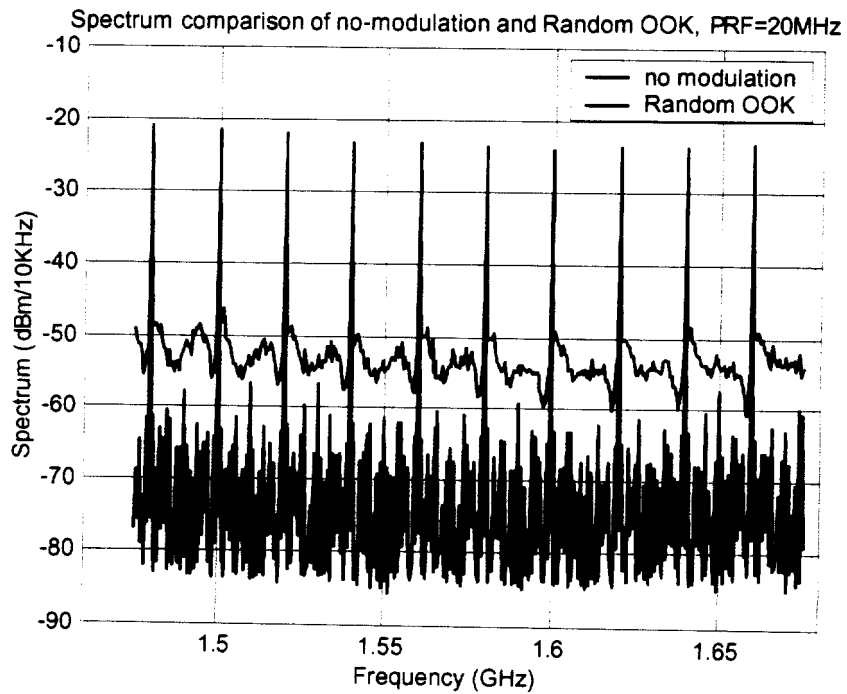


Figure 33: Spectrum Comparison between Random OOK and No-Modulation Cases

6.6 2 dB Back-Off

One issue that has not been addressed thus far in these results is what would occur if the UWB waveform is introduced at a different baseline broadband noise level? This aspect will be considered in further detail in the re-acquisition tests currently underway. However it is possible to provide a baseline case that can provide some insight into addressing this particular question.

Rather than decrease the noise power by 4 dB prior to adding the UWB signal, it is possible to decrease it by a different level and then introduce the UWB signal. In this case that noise back-off is 2 dB. The corresponding accuracy result for the two back-off traces is shown in Figure 34. This figure indicates that the accuracy curved traced out for the 2 dB back-off follows the line that would be expected from extrapolating the results of the 4 dB case. Note for this particular case, the internal smoothing time on the receiver was also increased, resulting in different scaling of the accuracy measure. This has been utilized in both the 4 dB and 2 dB curves in the plot so that the results are consistent. This provides some initial insight into addressing this issue, and it will be explored more thoroughly in later re-acquisition testing using the land receiver.

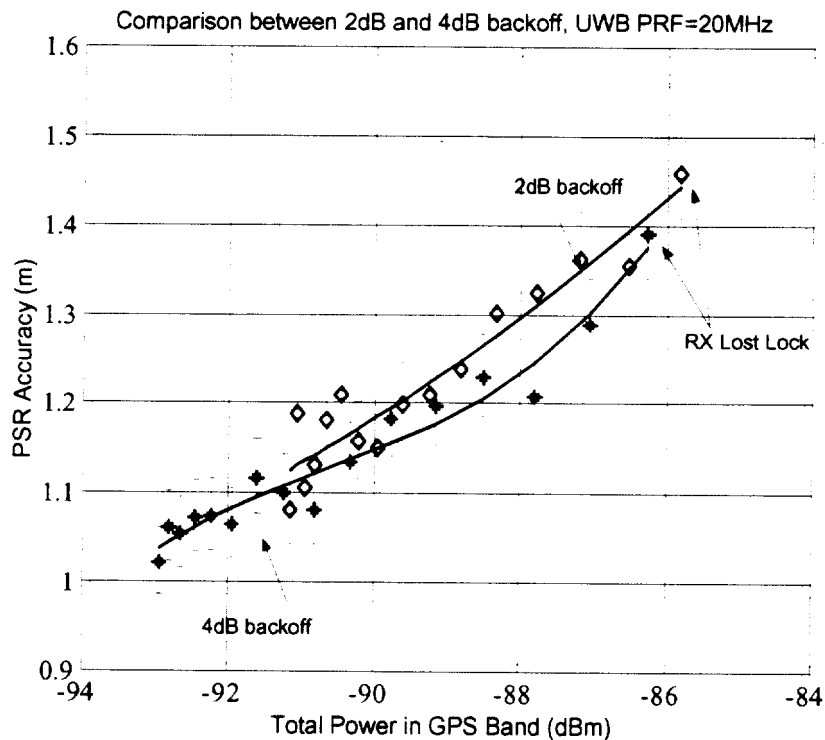


Figure 34: Accuracy Comparison between 4 dB and 2 dB Back-Off in Broadband Noise Power

7.0 Reacquisition Test Procedure for Land Receivers

The reacquisition time test procedure is described in the following two subsections. This test procedure is adapted from Section 2.5.6 of RTCA DO-229B, the *Minimum Operational Performance Standard (MOPS) for Avionics Using the Wide Area Augmentation System (WAAS)*. These tests assume that only one satellite is lost and needs to be reacquired. As such, the receiver is assumed to have a good estimate of its time offset relative to GPS time and the expected Doppler offset of the lost satellite. However, the receiver must search over all possible values of code phase.

Similar to the accuracy test, the reacquisition time test includes the following steps: calibration, normalization with broadband random noise only, UWB interference measurements, and reporting. Sections 7.1 and 7.2 detail the broadband random noise normalization and the UWB interference measurements. Further details are given in [10].

7.1 Broadband Random Noise Normalization

- 1) Set up the test equipment as shown in Figure 12. Connect the simulator clock to the receiver clock. This connection provides the time information to the receiver that is assumed in the reacquisition time tests described in Section 2.5.6 of the MOPS.
- 2) The GPS receiver is operated with the minimum rated received satellite signal level. Compensation is applied to adjust for room temperature, satellite simulator noise output, or the effects of a remote antenna preamplifier as needed. In other words, set the GPS power (C) to $-134.5 \text{ dBm} + G_{\text{LNA}}$ where G_{LNA} is the aggregate gain of any equipment that might nominally appear between the antenna and the receiver under test.
- 3) Add broadband random noise to the simulated GPS satellite signal at the receiver input. Set the center frequency of the broadband noise to 1575.42 MHz. The starting value is the RTCA/DO-229B MOPS level for initial acquisition. Adjust the broadband random noise power such that the noise power is $-103.5 \text{ dBm} + G_{\text{LNA}}$ as measured in the standard filter described earlier. The gain G_{LNA} accounts for the gain that nominally appears between the antenna and the receiver under test. As a rough check on power levels, measure the carrier to noise *density* (C/N_0) as reported by the receiver. This (C/N_0) should be approximately 33 dB-Hz.
- 4) Let the GPS receiver track the satellite and reach steady state (for at least 10 seconds).
- 5) Attenuate the GPS signal so that the receiver loses lock.
- 6) Introduce a 50 meter step in simulated pseudorange over 10 seconds while the signal is not being tracked by the receiver under test.
- 7) Remove the attenuation of the GPS signal and measure the time until the receiver reports code phase lock continuously for 10 seconds.
- 8) Repeat steps 4) through 7) until the sample size provides the confidence levels described above.

- 9) Increase the broadband random noise power by 1 dB and repeat steps 4) through 9) until the noise power (N_0) is slightly greater than the threshold power N_{REACQ}^* for the reacquisition time specification of 1 second.

7.2 Reacquisition Time Test with UWB Noise

- 1) Setup the test equipment as shown in Figure 12.
- 2) Set the noise power to 4 dB less than the threshold noise power (N_{REACQ}^*) determined in the broadband random noise tests described in Section 5.1.
- 3) Select one set of UWB signal parameters from the test matrix described earlier and set the UWB noise power (N_{UWB}) 10 dB below the broadband random noise power (N_0).
- 4) Let the GPS receiver track the satellite and reach steady state (for at least 10 seconds).
- 5) Attenuate the GPS signal so that the receiver loses lock.
- 6) Introduce a 50 meter step in simulated pseudorange over 10 seconds while the signal is not being tracked by the receiver under test.
- 7) Remove the attenuation of the GPS signal and measure the time until the receiver reports code phase lock continuously for 10 seconds.
- 8) Repeat steps 4) through 7) until the sample size provides the confidence levels described earlier for reacquisition time.
- 9) Increase the UWB noise power by 1 dB and repeat steps 4) through 9) until the total noise power ($N_0 + N_{UWB}$) is slightly greater than the power required to obtain a 1 second reacquisition time. Record the UWB power (N_{UWB}). Also find and record the reacquisition time when the total power (UWB plus broadband) equals the threshold power for broadband noise alone.
- 10) Change the UWB signal parameters to the next values in the test matrix and repeat steps 4) through 9) until all UWB signal parameters are exhausted.

8.0 Preliminary Land Receiver Results

The formal testing of the land receiver has recently commenced at Stanford University. This is expected to be the final phase of potential interference from UWB to GPS testing that will be conducted at Stanford University. Significant effort has been made to map the available hardware and its performance measures into the proposed test plan. This has been made possible through extensive testing and calibration of the test setup that has been conducted in parallel with the final data collections for the aviation receiver testing. It is possible that minor adjustments will be made in the testing procedure as deemed necessary by any possible equipment limitations.

It is expected that two different land receiver will be tested in parallel with respect to re-acquisition times. Testing is expected to be complete 31-December-2000, with a final report of the results ready approximately one month later.

Very preliminary results demonstrate a dependency on the resulting UWB spectral lines and increased broadband noise floor, similar to that observed for the aviation receiver accuracy testing. Full quantitative results will be made available in the report written for this phase of testing being conducted at Stanford University.

9.0 Summary and Conclusions

For a single aviation-grade GPS receiver, Stanford University has developed a test plan to study the impact of UWB transmissions on GPS users by relating it to the impact of broadband noise. By carrying out these tests, we have demonstrated how the impact of UWB interference on GPS depends on several sets of UWB signal parameters, including PRFs, duty cycles, on-times, and modulation variations. The resulting data from these tests will be made available through our sponsor, the Department of Transportation. The impact of UWB is strongly dependent on the UWB pulse repetition rate and the presence and location of UWB spectral lines relative to GPS. To a large degree, the impact of UWB can be explained (and predicted) by examining UWB pulse repetition frequency and where the UWB spectral lines are relative to the GPS spectrum around L1 and the power of these lines.

When the UWB PRF is low, specifically when the post-filter UWB pulses occupy less than 10% duty cycle (as in the 100 kHz case), UWB has less impact on GPS receivers than does broadband noise of the same power level. This is due to the fact that the filtered UWB pulses interfere for only a small fraction of the time, and GPS receivers are very robust in the presence of such low duty cycle interference. When the PRF is this low, UWB signals are less damaging than an equal amount of broadband noise. Moreover, the impact on GPS is less sensitive to small variations in PRF or modulation. However if more than one UWB signal is present, then this finding will likely not hold. When multiple UWB signals arrive asynchronously, then the PRF of concern is the aggregate PRF – not any individual PRF. If this aggregate pulse stream occupies more than a 10% duty cycle after the GPS receiver filter, then we speculate that UWB interference will be much higher.

When the PRF is high (the filtered UWB pulses occupy more than 10% duty cycle), then the effects are very different. Specifically, we observed many cases where the impact of UWB on GPS accuracy is worse than broadband noise, and some of these cases make the GPS receiver lose lock at very low power levels. When the UWB PRF is high (e.g., above 5 MHz), a small variation in PRF (which could easily be caused by clock imperfections) makes a large difference on the impact of interference to the GPS receiver. These variations in impacts on GPS are well-explained by the locations of the UWB spectral lines relative to GPS. Since the impact of small variations in the location of these lines can lead to severe consequences to GPS, UWB signals should avoid having powerful spectral lines of this type. Note that these tests were limited by our pulser to a maximum PRF of 20 MHz; thus there was always at least one spectral line in the GPS L1 band.

UWB signals can use pseudorandom modulation to reduce the impact of the spectral lines. Our tests used both pseudorandom pulse position modulation (PPM) and on-off-keying (OOK). In the modulated cases that we tested, the UWB spectral lines did not completely disappear. In other words, the impact of UWB did not become entirely “white-noise-like”. Our test waveforms had different spectral-line characteristics, and therefore result in varying impacts on GPS:

1. Random OOK does not change the location of spectral lines relative to the no-modulation case with the same PRF. It only reduces the power of the spectral lines by a few dB.
2. Multiple-position random PPM makes the larger spectral lines more sparsely spread and generates more small lines closer to each other.
3. Two-position random PPM changes the shape of the spectral noise floor, while the spectral lines remain at the same locations they are in without modulation.

Our tests showed a high sensitivity to the spectral lines near the GPS band. From our tests, the presence of spectral lines in the main lobe of the GPS spectrum for an unmodulated UWB signal at 100% duty cycle with PRF near 20 MHz translates into a gap of about 9 dB between the power level at which lock is lost with UWB and the higher power level where lock is lost under broadband noise only. This gap is reduced by varying degrees by reducing the nominal PRF or duty cycle or by adding random PPM or OOK modulation, but it is not removed entirely.

If very carefully designed, pseudorandom modulation methods may be able to render UWB interference equivalent to broadband noise (e.g., [12]). We plan to examine some of these techniques in our next round of tests to determine to what degree these spikes can be further reduced. However, even if a scheme is found that guarantees removal of the spectral lines, the best that can be achieved is to render UWB equivalent to broadband noise. This is demonstrated by the results of the cases without threatening spectral lines – the slope of the accuracy curves with UWB added approximately match those of the broadband-noise-only line. However, this possibility simply means that the UWB interference effect is easy to analyze – it does not mean that the interference is non-existent.

Testing has also commenced on a land receiver to determine its ability to re-acquire the GPS signal in the presence of UWB. The procedure for such testing is also described in the original test plan. Although this testing has just been initiated, preliminary results show similar sensitivities as those experience for the accuracy testing of the aviation receiver. The presence of distinct spectral lines hinders re-acquisition just as they resulting in early loss of locks in the aviation testing. Results for the land receiver will be presented as they become available.

The impact of UWB on GPS varies considerably with UWB signal characteristics, but it is possible to quantify the difference between UWB interference and broadband noise. Moreover, it is possible to understand how that equivalence depends on the UWB signals parameters. In particular, UWB signals are less damaging than broadband noise when very low UWB PRFs are used and only a single UWB emitter is interfering. On the other hand, UWB signals are significantly more damaging than broadband noise when large spectral spikes fall in the GPS band. To advance our current understanding, Stanford is now pursuing further tests with commercial land receivers and will support tests of a second aviation receiver. At the same time, standards boards such as RTCA SC-159 WG-6 are devising specific UWB-GPS interference scenarios in which our test results will be utilized.

10.0 References

1. *Assessment of Radio Frequency Interference Relevant to the GNSS*, January 27, 1997 (RTCA DO-235).
2. *Minimum Aviation Performance Standards for the Local Area Augmentation System*, September 28, 1998 (RTCA/DO-245).
3. *Minimum Operational Performance Standards for Global Positioning System/Wide Area Augmentation System Airborne Equipment*, October 6, 1999 (RTCA DO-229B or the GPS/WAAS MOPS).
4. *Minimum Operational Performance Standards for GPS Local Area Augmentation System Airborne Equipment*, January 11, 2000, (RTCA DO-253 or the GPS/LAAS MOPS).
5. *Technical and Performance Characteristics of Current and Planned RNSS (space-to-earth) and ARNS Receivers to be Considered in Interference Studies in the 1559 to 1610MHz*, International Telecommunications Union (ITU) Document 8/83-E, April 29, 1999
6. International Civil Aviation Organization (ICAO) Global Navigation Satellite System Panel (GNSSP) SARPs, *Resistance to Interference Section B.3.7*
7. *Technical Standard Order C129, Airborne Supplemental Navigation Equipment Using the Global Positioning System (GPS)*, TSO C129, USDOT Federal Aviation Administration, December 1992.
8. *Global Positioning System - Standard Position System Signal Specification*; 2nd Edition; June 2, 1995.
9. G. Aiello, G. Rogerson, Per Enge, "Preliminary Assessment of Interference Between Ultra-Wideband Transmitters and the Global Positioning System: A Cooperative Study," *Proceedings of the 2000 Institute of Navigation National Technical Meeting*, Anaheim, CA., Jan. 26-28, 2000, pp. 28-35
10. M. Luo, D. Akos, S. Pullen, P. Enge "Potential Interference to GPS from UWB Transmitters: Test Plan, Phase I," Stanford University, Version 4.5, May 1, 2000.
11. B. Parkinson, J. Spilker, P. Axelrad, P. Enge, *Global Positioning System: Theory and Applications*, Vol. 1, pp. 97-114, American Institute of Aeronautics and Astronautics, Inc., ISBN 1-56347-106-X, 1996.
12. R. Fontana, "A Note on Power Spectral Density Calculations for Jittered Pulse Trains," Germantown, MD., Multispectral Solutions, Inc., <http://www.multispectral.com/presentations.html>, 2000.